RKKY in half-filled bipartite lattices: Graphene as an example

Saeed Saremi
Department of Physics, Massachusetts Institute of Technology, Cambridge, Massachusetts 02139, USA
(Received 24 May 2007; published 21 November 2007)

We first present a simple proof that for any bipartite lattice at half filling, the RKKY interaction is antiferromagnetic between impurities on opposite (i.e., *A* and *B*) sublattices and is ferromagnetic between impurities on the same sublattices. This result is valid on all length scales. We then focus on the honeycomb lattice and examine the theorem in the long distance limit by performing the low energy calculation using Dirac electrons. To find the universal (cutoff-free) result, we perform the calculation in smooth cutoff schemes, as we show that the calculation based on a sharp cutoff leads to wrong results. We also find the long distance behavior of the RKKY interaction between "plaquette" impurities in both coherent and incoherent regimes.

DOI: 10.1103/PhysRevB.76.184430 PACS number(s): 75.20.Hr, 75.10.Jm, 75.30.Ds, 75.10.Lp

I. INTRODUCTION

The Ruderman-Kittel-Kasuya-Yosida (RKKY) interaction between magnetic impurities in a metallic environment plays a crucial role in the way magnetic impurities order both in the dilute and the Kondo lattice limits.[1] Perfect nesting of the Fermi surface provides a mechanism for ordering due to the divergence of the spin susceptibility at the nesting wave vector.[2] The square lattice at half filling provides the best known example for perfect nesting and the consequent (π,π) antiferromagnetic ordering of the magnetic impurities. The *minimal* form of nesting appears in the undoped single layer of graphite[3] where the Fermi surface shrinks to two Dirac points. However, we show that the particle-hole symmetry provides another mechanism for ordering of the magnetic impurities in a metallic environment on *all* length scales. This result can be applied to the undoped graphene and is of value since low energy calculations are only valid in the long distance limit. Furthermore, this result provides a test for the low energy calculations and we show that the calculation based on a *sharp* cutoff fails this test. We also study the RKKY interaction between localized spins with more complicated Kondo interactions. Interestingly, the behavior of the RKKY interaction is qualitatively different for different types of magnetic impurities. It will be interesting to see which one of the scenarios we considered—if not all—can be realized in the laboratory.

The organization of the paper is as follows. In Sec. II, we consider the simplest Kondo perturbation, where the impurity is localized at a lattice site, and only has an *on-site* Kondo interaction with the conduction electron spin. We prove a theorem for the RKKY interaction between these "site impurities" in bipartite lattices with hopping between opposite *AB* sublattices at half filling. The result is that the sign of the RKKY interaction depends *only* on whether the impurities are localized at opposite sublattices (antiferromagnetic) or on the same sublattices (ferromagnetic). The sign is dictated by particle-hole symmetry and is thus valid on all length scales.

Section III focuses on the half-filled honeycomb lattice with nearest neighbor hopping and examines the above theorem in the long distance limit. We do a low energy calculation for the RKKY exchange in different cutoff schemes to obtain the long distance behavior of the exchange. As will be explained, due to the nature of the singularity of the spin susceptibility near the Dirac nodes, the use of sharp cutoff is inappropriate. We do the sharp cutoff calculation to demonstrate this fact. We then examine two smooth cutoffs to find the long distance behavior of the exchange. *Two* cutoffs are considered to make sure that the calculation is cutoff independent. They both lead to the same answer in the long distance limit.

It is important to note that although both antiferromagnetic and ferromagnetic exchanges have the same algebraic decay power in the long distance limit, the coefficients of their decays are not the same. Furthermore, focusing on the RKKY in a single class (i.e., the same or opposite sublattices), there is also magnitude "oscillations" of the form $\cos(2\boldsymbol{k}_D\cdot(\boldsymbol{R}-\boldsymbol{R}'))$ due to the nonanalyticity of the susceptibility at the wave vector connecting the two nodes.

In Sec. III B, we discuss the extension of the RKKY between site impurities to more general cases. In particular, we find the qualitative behavior of the RKKY for magnetic impurities sitting at the center of the hexagons of the honeycomb lattice. We distinguish this type of impurity by calling it *plaquette* impurity (vs site impurity). In writing the Kondo perturbation, these plaquette impurities can couple coherently or incoherently with the conduction electrons. We find that, for incoherent Kondo couplings, the RKKY exchange between plaquette impurities is *always antiferromagnetic*.

We then obtain the RKKY behavior for plaquette impurities when they have a *coherent* Kondo interaction with the conduction electrons around the plaquette. We find that, due to a nontrivial phase cancellation, the $1/R^3$ algebraic tail, present in all other situations we considered, vanishes.

We conclude by summarizing our results and mentioning our disagreements—specially in the *sign* of the RKKY interaction—with other attempts[4,5] made in calculating the RKKY interaction in graphene. We also discuss the direct implication of this paper for the Kondo lattice model on the honeycomb lattice.

II. LATTICE RESULTS

To establish notation, we quickly review the RKKY interaction.[6] Imagine putting two test localized spins *S* at

lattice sites i and $j(i \neq j)$ and assume they have a small on-site spin exchange interaction with the conduction electron spin s. This perturbs the free hopping Hamiltonian

$$\hat{H} = -t \sum_{\langle ij \rangle, a} (\hat{c}^{\dagger}_{ia} \hat{c}_{ja} + \text{H.c.}) \tag{1}$$

by

$$\delta \hat{H} = \mathrm{j}(\boldsymbol{S}_i \cdot \boldsymbol{s}_i + \boldsymbol{S}_j \cdot \boldsymbol{s}_j) \quad (|\mathrm{j}| \ll t). \tag{2}$$

In perturbation theory, the leading interaction induced by this term is

$$\hat{H}_{\mathrm{RKKY}} = J_{ij} \boldsymbol{S}_i \cdot \boldsymbol{S}_j, \tag{3}$$

where J_{ij} is given by

$$J_{ij} = -\mathrm{j}^2 \int d\tau \langle s^-_i(\tau) s^+_j(0) \rangle. \tag{4}$$

To be precise, J_{ij} is the coefficient of the $S^+_i S^-_j$. However, due to the SU(2) flavor symmetry of the unperturbed Hamiltonian, J^{-+}_{ij}, J^{+-}_{ij}, and J^{zz}_{ij} are all equal. It is also understood that this is the static (imaginary-time-averaged) part of the RKKY interaction.

Nearest neighbor hopping on a bipartite lattice can be viewed as a special case of hopping between A and B sublattices. The particle-hole transformation

$$c_{ia}(\tau) \to (-1)^i \bar{c}_{ia}(\tau), \tag{5}$$

where c and its conjugate $\bar{c}$ are the Grassmann fields, leaves the Lagrangian invariant. Lattice sites are labeled such that i is odd on A sublattices and even on B sublattices. This transformation sends the chemical potential μ to $-\mu$. However, at half filling, $\mu=0$ and the particle-hole transformation is a symmetry of the partition function.

Using Wick's theorem, we have

$$J_{ij} = -\mathrm{j}^2 \int d\tau \langle \bar{c}_{i\downarrow}(\tau) c_{j\downarrow}(0) \rangle \langle c_{i\uparrow}(\tau) \bar{c}_{j\uparrow}(0) \rangle. \tag{6}$$

We drop the spin indices from now on since the Green's functions do not depend on the spin flavor. Since the ground state is particle-hole symmetric, the particle-hole symmetry of the Lagrangian implies

$$\langle c_i(\tau) \bar{c}_j(0) \rangle = (-1)^{i+j} \langle \bar{c}_i(\tau) c_j(0) \rangle. \tag{7}$$

The above relation immediately results in

$$J_{ij} = -\mathrm{j}^2 (-1)^{i+j} \int d\tau G_{ij}(\tau)^2, \tag{8}$$

where $G_{ij}(\tau)$ is defined to be

$$G_{ij}(\tau) = \langle \bar{c}_i(\tau) c_j(0) \rangle. \tag{9}$$

In addition, $G_{ij}(\tau)$ is real, as the space-time matrix connecting the Grassmann variables is real. Therefore,

$$\frac{J_{ij}}{|J_{ij}|} = (-1)^{i+j+1}. \tag{10}$$

The same result is obtained if the Hamiltonian of Eq. (1) contains more general hopping terms, but only between AB sublattices. In summary, for any bipartite lattice at half filling, with hopping only between AB sublattices, the RKKY interaction is antiferromagnetic between impurities on opposite sublattices and is ferromagnetic between impurities on the same sublattices.

III. LOW ENERGY CALCULATION

Next, we focus on the honeycomb lattice with nearest neighbor hopping and examine the theorem we proved in the long distance limit. The low energy theory is known to be governed by a $2+1$ dimensional Dirac action containing the Dirac spinors—with internal A-B flavor—residing near the two independent nodes $\pm \boldsymbol{k}_D$. Being "near" the nodes is formulated by introducing a momentum cutoff and a cutoff scheme in the calculations.

The division of the honeycomb lattice to A and B sublattices is a necessity, as the Bravais lattice has a basis with two sites. Let us set the distance between the nearest neighbor sites to be 1. In the limit $|\boldsymbol{R}-\boldsymbol{R}'| \gg 1$, the RKKY interaction $J_{AB}(\boldsymbol{R}-\boldsymbol{R}')$ is calculated by Fourier transforming Eq. (6) and constraining the momenta to be near the Dirac nodes:

$$J_{AB}(\boldsymbol{R}-\boldsymbol{R}') \approx -\mathrm{j}^2 \sum_{D,D'} \int \frac{d^2\boldsymbol{q}}{(2\pi)^2} e^{i\boldsymbol{q}\cdot(\boldsymbol{R}-\boldsymbol{R}')} \times e^{i(D-D')\boldsymbol{k}_D\cdot(\boldsymbol{R}-\boldsymbol{R}')} \chi^{DD'}_{AB}(q_0=0,\boldsymbol{q}) \mathcal{C}_\Lambda(|\boldsymbol{q}|). \tag{11}$$

Here, $\boldsymbol{R}$ and $\boldsymbol{R}'$ refer to the Bravais lattice vectors. D and D' are either $+1$ or -1. They denote near which Dirac nodes $\pm \boldsymbol{k}_D$ the (space) momenta reside. $\Lambda \ll 1$ is the cutoff and $\mathcal{C}_\Lambda(|\boldsymbol{q}|)$ is a function that takes care of cutting off the momentum. Three examples for $\mathcal{C}_\Lambda(|\boldsymbol{q}|)$ will be given below.

$\chi^{DD'}_{AB}(q)$ is given diagrammatically by

$$\chi^{\mathrm{DD'}}_{\mathrm{AB}}(q) = \int \frac{d^3k}{(2\pi)^3}$$

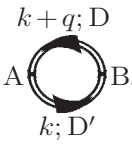

(12)

We use the continuum limit "translation" of the fields in terms of microscopic variables provided by Eqs. (45) and (50) of Ref. 7 to obtain

$$\chi^{++}_{AB}(0,\boldsymbol{q}) = \frac{3|\boldsymbol{q}|}{64}, \tag{13}$$

$$\chi^{--}_{AB}(0,\boldsymbol{q}) = \chi^{++}_{AB}(\boldsymbol{q}), \tag{14}$$

$$\chi^{+-}_{AB}(0,\boldsymbol{q}) = \frac{1}{64|\boldsymbol{q}|}(q_x + iq_y)^2, \tag{15}$$

$$\chi^{-+}_{AB}(0,\boldsymbol{q}) = \chi^{+-}_{AB}(\boldsymbol{q})^*. \tag{16}$$

In the above calculations, the Dirac dispersion velocity v_c is set to be 1 by scaling the space dimensions.

To calculate $J_{AB}(\boldsymbol{R}-\boldsymbol{R}')$, we examine the following cutoff functions:

$$\mathcal{C}^1_\Lambda(|\boldsymbol{q}|) = \theta(\Lambda - |\boldsymbol{q}|), \tag{17}$$

$$\mathcal{C}^2_\Lambda(|\boldsymbol{q}|) = e^{-|\boldsymbol{q}|/\Lambda}, \tag{18}$$

$$\mathcal{C}^3_\Lambda(|\boldsymbol{q}|) = e^{-\boldsymbol{q}^2/\Lambda^2}, \tag{19}$$

where θ is the step function.

The issue is that the susceptibility is dominated by larger values of $|\boldsymbol{q}|$, and the decay that phase integration causes, in the sharp cutoff scheme, is not strong enough to compensate that. This issue becomes more severe in the continuum limit $\Lambda|\boldsymbol{R}-\boldsymbol{R}'|\to\infty$.

Since small $|\boldsymbol{q}|$ *must* dominate the large distance behavior, we should adopt a different cutoff scheme than the sharp cutoff. For the same reason, the answer should be universal, not just the power of decay but also its coefficient. That is why we examine two different cutoff schemes $\mathcal{C}^2_\Lambda$ and $\mathcal{C}^3_\Lambda$ to make sure that we find the cutoff independent answer.

A. Examining different cutoffs

Next, we do the calculations for the three cutoff schemes we have considered. We first show explicitly that the sharp cutoff is inappropriate. We then find the universal answer for the RKKY interaction using the smooth cutoffs $\mathcal{C}^2_\Lambda$ and $\mathcal{C}^3_\Lambda$.

1. Sharp cutoff

Doing the integral of Eq. (11) for $D=D'=+1$ using $\mathcal{C}^1_\Lambda$ results in

$$J^{++}_{AB}(\boldsymbol{R}-\boldsymbol{R}') \propto \frac{1}{|\boldsymbol{R}-\boldsymbol{R}'|^3}\int_0^{\Lambda|\boldsymbol{R}-\boldsymbol{R}'|} dx x^2 J_0(x). \tag{20}$$

The Bessel function $J_0(x)$ is obtained by doing the angular integration. The integrand in the above equation is a widely oscillating function in the limit $\Lambda|\boldsymbol{R}-\boldsymbol{R}'|\gg 1$. Using the asymptotic form for $J_0(x)$, one easily obtains

$$J^{++}_{AB}(\boldsymbol{R}-\boldsymbol{R}') \propto \frac{1}{|\boldsymbol{R}-\boldsymbol{R}'|^{3/2}}\sin\left(\Lambda|\boldsymbol{R}-\boldsymbol{R}'| - \frac{\pi}{4}\right). \tag{21}$$

The *changed scaling form*, as well as the sine oscillations, is generated by the sharp cutoff in momentum space. The sine causes sign oscillations in contradiction to the theorem we proved in Sec. I, thus making the sharp cutoff inappropriate. Again even without the theorem; we can see that the integral is dominated by larger values of $|\boldsymbol{q}|$, and that is enough to make the sharp cutoff inappropriate.

2. Smooth cutoffs

Because of this issue, we use the smooth cutoffs given by Eqs. (18) and (19). As expected, $\mathcal{C}^2_\Lambda$ and $\mathcal{C}^3_\Lambda$ both lead to the same result in the continuum limit. The few integrals needed for this calculation are given in the Appendix. The final result is

$$J_{AB}(\boldsymbol{R}-\boldsymbol{R}') \approx \frac{3\mathrm{j}^2}{64\pi}\frac{1+\cos(2\boldsymbol{k}_D\cdot(\boldsymbol{R}-\boldsymbol{R}'))}{|\boldsymbol{R}-\boldsymbol{R}'|^3}, \tag{22}$$

where $\approx$ is used since it is the continuum limit $\Lambda|\boldsymbol{R}-\boldsymbol{R}'|\to\infty$ result. We also mention the results for $\chi^{DD'}_{AA}$:

$$\chi^{DD'}_{AA}(0,\boldsymbol{q}) = -\frac{|\boldsymbol{q}|}{64}. \tag{23}$$

The same cutoff functions $\mathcal{C}^2_\Lambda$ and $\mathcal{C}^3_\Lambda$ result in

$$J_{AA}(\boldsymbol{R}-\boldsymbol{R}') \approx \frac{-\mathrm{j}^2}{64\pi}\frac{1+\cos(2\boldsymbol{k}_D\cdot(\boldsymbol{R}-\boldsymbol{R}'))}{|\boldsymbol{R}-\boldsymbol{R}'|^3}. \tag{24}$$

B. RKKY for plaquette impurities

The perturbation we considered in Eq. (2) is the simplest Kondo perturbation one can consider. In general, the localized spin could have interactions with several conduction electrons. In the honeycomb lattice, this can be realized experimentally by having the localized spins near the center of the graphene's hexagons.

To study these situations, let us consider a slight change of notations in denoting the localized spins. The Greek letter index $\boldsymbol{S}^\alpha$ is used to denote the localized spins in these situations. This is in contrast to the notation $\boldsymbol{S}_i$ for the on-site perturbations we started this paper with. To establish notation, we first consider the simpler theoretical problem in which the impurity has an incoherent Kondo interaction with the conduction electron spins around the plaquette. The perturbation to the free hopping Hamiltonian is then

$$\delta\hat{H} = \mathrm{j}T^\alpha_i \boldsymbol{S}^\alpha\cdot\boldsymbol{s}_i \quad (|\mathrm{j}| \ll t), \tag{25}$$

where the sum over α (localized spins) and i (lattice sites) is understood. We assume that $\boldsymbol{S}^\alpha$ has interactions with only a few $\boldsymbol{s}_i$'s. For example, if $\boldsymbol{S}^\alpha$ is located near the center of a hexagon in the honeycomb lattice, we assume that T^α_i has only six nonzero elements, corresponding to the sites surrounding the hexagon.

The RKKY interaction between $\boldsymbol{S}^\alpha$ and $\boldsymbol{S}^\beta$ is

$$J^{\alpha\beta}\boldsymbol{S}^\alpha\cdot\boldsymbol{S}^\beta, \tag{26}$$

where $J^{\alpha\beta}$ is given by

$$J^{\alpha\beta} = T^\alpha_i T^\beta_j J_{ij}, \tag{27}$$

and J_{ij} is given by Eq. (4).

To be concrete, let us consider the honeycomb lattice and imagine that the localized spins are located at the center of the hexagons and are widely separated. We consider the "s-wave" model in which the nonzero elements of T^α_i are all 1. $J^{\alpha\beta}(\boldsymbol{R}-\boldsymbol{R}')$ is then given by summing over 36 terms that are given by either Eq. (22) or Eq. (24). Since A and B sites surrounding the hexagons belong to different Bravais lattice sites, the separations in Eq. (22) or Eq. (24) are, in general, given by different $\boldsymbol{R}-\boldsymbol{R}'$, e.g., $\boldsymbol{R}-\boldsymbol{R}'\pm\boldsymbol{a}_1$, $\boldsymbol{R}-\boldsymbol{R}'\pm\boldsymbol{a}_2$, etc. Here, $\boldsymbol{a}_1$ and $\boldsymbol{a}_2$ are the primitive vectors of the Bravais lattice. However, in the long distance limit, all the decay factors can be replaced by $1/|\boldsymbol{R}-\boldsymbol{R}'|^3$.

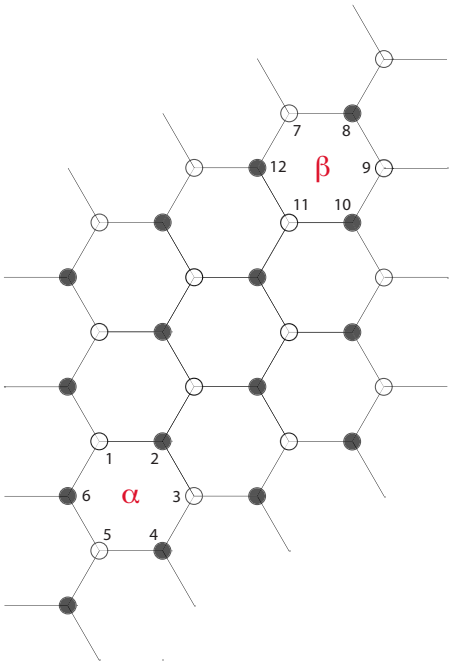

FIG. 1. (Color online) The honeycomb lattice. A sublattice is denoted by odd (empty) sites. Plaquettes α and β and the sites surrounding them are labeled. Fixing i on any site and running $j \in A$ (around a plaquette) result in $\{0,1,2\}$ patterns for $O_{ij}=m_i+n_i-m_j-n_j \pmod 3$. The same set is obtained by scanning $j \in B$. Thus, this procedure results in the set $\{-1/2,-1/2,1\}$ for $\cos(2\boldsymbol{k}_D\cdot\boldsymbol{R}_{ij})$ and $\cos(\boldsymbol{k}_D\cdot\boldsymbol{R}_{ij})$.

Treating the cosine is a bit more delicate as $\cos(2\boldsymbol{k}_D\cdot(\boldsymbol{R}-\boldsymbol{R}'))$ is not a smooth function. It is straightforward to show that $\cos(2\boldsymbol{k}_D\cdot\boldsymbol{R})$ is either $-1/2$ or 1. If we decompose $\boldsymbol{R}$ into the primitive vectors

$$\boldsymbol{a}_1 = (3/2, \sqrt{3}/2), \tag{28}$$

$$\boldsymbol{a}_2 = (0, -\sqrt{3}), \tag{29}$$

$$\boldsymbol{R} = m\boldsymbol{a}_1 + n\boldsymbol{a}_2, \tag{30}$$

together with

$$\boldsymbol{k}_D = \left(0, \frac{4\pi}{3\sqrt{3}}\right), \tag{31}$$

one finds

$$\cos(2\boldsymbol{k}_D\cdot\boldsymbol{R}) = \cos(4\pi(m+n)/3). \tag{32}$$

However, as we explain, this complication does not come into play and the RKKY exchange between the plaquette impurities we have considered is always antiferromagnetic.

To see this, one has to label the sites around the two hexagons in terms of (m,n) pairs. It is straightforward to see that the set of

$$O = m + n - m' - n' \pmod 3 \tag{33}$$

for AA and BB sublattices is the same as the set for opposite AB sublattices; thus, antiferromagnetism prevails. It can is also found (see Fig. 1) that these sets will be grouped to $\{0,1,2\}$. Therefore, the cosine contributions of Eqs. (22) and (24), when summed over the sites around two plaquettes, vanish; to the leading order, $J^{\alpha\beta}(\boldsymbol{R}-\boldsymbol{R}')$ is given by

$$J^{\alpha\beta}(\boldsymbol{R}-\boldsymbol{R}') \approx \frac{9\mathrm{j}^2}{16\pi}\frac{1}{|\boldsymbol{R}-\boldsymbol{R}'|^3}. \tag{34}$$

To summarize, the RKKY exchange for plaquette impurities (in the long distance limit) is always antiferromagnetic. Since the centers of the hexagons form a triangular lattice, the RKKY exchange for the widely separated plaquette impurities is frustrated.

We also mention the results for the RKKY interaction between a plaquette impurity and a site impurity. Again, the $\cos(2\boldsymbol{k}_D\cdot(\boldsymbol{R}-\boldsymbol{R}'))$, present in the RKKY for site impurities, when summed over the plaquette, vanishes. The final result is given by

$$J_A^{\alpha}(\boldsymbol{R}-\boldsymbol{R}') \approx \frac{3\mathrm{j}^2}{32\pi}\frac{1}{|\boldsymbol{R}-\boldsymbol{R}'|^3}. \tag{35}$$

The same result is obtained when the site impurity is on a B sublattice.

We finally extend the incoherent Kondo coupling of plaquette impurities with the conduction electron given by Eq. (25) to the coherent one. The coherent Kondo perturbation is more physical. It can be justified by going back to the origin of the Kondo model, i.e., the Anderson model. In the coherent Kondo coupling, the S^{α} has a Kondo interaction with a coherent sum of conduction electron spin. The Kondo perturbation is then given by

$$\delta\hat{H} = \mathrm{j}\boldsymbol{S}^{\alpha}\cdot\boldsymbol{s}_{\alpha} \quad (|\mathrm{j}| \ll t), \tag{36}$$

where $\boldsymbol{s}_{\alpha}$ is a coherent sum of the conduction electron spins around plaquette α, e.g., s_{α}^{+} is given by

$$s_{\alpha}^{+} = \frac{1}{6}\sum_{i,j\in\mathcal{P}^{\alpha}} \hat{c}_{i\uparrow}^{\dagger}\hat{c}_{j\downarrow}, \tag{37}$$

and $\mathcal{P}^{\alpha}$ is the set of sites surrounding plaquette α. The susceptibility needed in these calculations carries four sublattice indices:

$$\chi_{\mathrm{ikjl}}^{\mathrm{DD}'}(q) = \int \frac{d^3k}{(2\pi)^3}$$

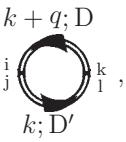

, (38)

since in calculating $\langle s_{\alpha}^{+}s_{\beta}^{-}\rangle$, four sites $\{i,j,k,l\}$ are involved. Here, $i,j\in\mathcal{P}^{\alpha}$ and $k,l\in\mathcal{P}^{\beta}$. We avoided using a separate notation for sublattice indices in $\chi_{ikjl}^{DD'}(q)$, e.g., i in $\chi_{ikjl}^{DD'}(q)$ should be replaced with A if $i\in A$, etc. $J_{*}^{\alpha\beta}$ is then given by

$$J_{*}^{\alpha\beta} \approx -\mathrm{j}^2 \sum_{i,j\in\mathcal{P}^{\alpha}} \sum_{k,l\in\mathcal{P}^{\beta}} \sum_{D,D'} \int \frac{d^2\boldsymbol{q}}{(2\pi)^2} e^{i(\boldsymbol{q}+D\boldsymbol{k}_D)\cdot(\boldsymbol{R}_i-\boldsymbol{R}_k)}$$
$$\times e^{iD'\boldsymbol{k}_{D'}\cdot(\boldsymbol{R}_l-\boldsymbol{R}_j)}\chi_{ikjl}^{DD'}(q_0=0,\boldsymbol{q})\mathcal{C}_{\Lambda}(|\boldsymbol{q}|). \tag{39}$$

Asterisk (*) is used to make the distinction between the

coherent RKKY and the incoherent RKKY of Eq. (34).

It is straightforward to find that

$$\sum_{i,j\in\mathcal{P}^{\alpha}k,l\in\mathcal{P}^{\beta}}{}' \sum_{D,D'}{}' \sum e^{iD\boldsymbol{k}_D\cdot(\boldsymbol{R}_i-\boldsymbol{R}_k)}e^{iD'\boldsymbol{k}_{D'}\cdot(\boldsymbol{R}_l-\boldsymbol{R}_j)}=0, \tag{40}$$

where Σ' is used to denote that in summing over indices, each site index is restricted to be in a *single* sublattice. This is just an immediate result of the observation we made in the previous discussions and is explained briefly in the caption of Fig. 1. Since

$$\int \frac{d^2\boldsymbol{q}}{(2\pi)^2}e^{i\boldsymbol{q}\cdot(\boldsymbol{R}_i-\boldsymbol{R}_k)}\chi_{ikjl}^{DD'}(q_0=0,\boldsymbol{q})\mathcal{C}_{\Lambda}(|\boldsymbol{q}|) \tag{41}$$

is independent of D and D', Eq. (40) implies that the $1/|\boldsymbol{R}-\boldsymbol{R}'|^3$ dependence of $J_*^{\alpha\beta}$ vanishes:

$$J_*^{\alpha\beta}(\boldsymbol{R}-\boldsymbol{R}')=0+\mathcal{O}(1/|\boldsymbol{R}-\boldsymbol{R}'|^4). \tag{42}$$

Note that the *incoherent* Kondo perturbation corresponds to $i=j$ and $k=l$. The sum in Eq. (40), with this further constraint, does not factor out and it does not vanish [see Eq. (34)].

IV. CONCLUSIONS

We first proved that the particle-hole symmetry for bipartite lattices determines the sign of RKKY interaction between site impurities on all length scales. Second, the nature of the singularity of the spin susceptibility in graphene invalidates the use of sharp cutoff. In the sharp cutoff scheme, the main contribution for the RKKY interaction comes from the large momenta, thus invalidating the low energy theory.

We then studied the RKKY between plaquette impurities and also between a plaquette impurity and a site impurity. We first considered the simpler case of having an incoherent Kondo perturbation. For these incoherent perturbations, the RKKY involving plaquette impurities (in the long distance limit) always ends up being *antiferromagnetic*. This comes from the fact that in mediating RKKY, the contributions of electrons on opposite sublattices dominate the contributions from the same sublattices [Eq. (22) vs Eq. (24)]. If they had equal strengths, the $1/|\boldsymbol{R}-\boldsymbol{R}'|^3$ dependence of the RKKY involving plaquette impurities would have vanished.

We then focused on plaquette impurities in the coherent Kondo interaction regime. We found that the $1/R^3$ algebraic tail of the RKKY, present in all other situations we considered, vanishes. More work needs to be done for finding the leading contribution for the RKKY in this case.

In terms of the *magnitude* of the RKKY in the long distance limit, our results can be summarized symbolically as

$$|J^{\alpha\beta}|>|J_A^{\alpha}|>|J_{AB}|>|J_{AA}|\gg|J_*^{\alpha\beta}|. \tag{43}$$

There had been other attempts in calculating RKKY in graphene.[4,5] They also observed a $1/R^3$ dependence for the RKKY. However, it was claimed that the RKKY is *always* ferromagnetic due to graphene's "semimetalic properties." Based on our result, this *may* only happen for the plaquette impurities with coherent Kondo interactions [see Eq. (42)], and in that case, the RKKY decay is faster than $1/R^3$.

Finally, we mention the implications of this paper for the Kondo lattice model on the honeycomb lattice. We started the study of the Kondo-Heisenberg model on the honeycomb lattice[7] with the hope of finding the first examples of algebraic spin liquid phase in the presence of a semimetal, or a Kondo-insulator–Néel deconfined quantum critical point.[8] Based on the result of Sec. II, $J_H>0$ *will be generated* in the small J_K limit of the Kondo lattice model,

$$\hat{H}=-t\sum_{\langle ij\rangle,a}(\hat{c}_i^{a\dagger}\hat{c}_j^a+\text{H.c.})+J_K\sum_i \boldsymbol{s}_i\cdot\boldsymbol{S}_i, \tag{44}$$

and in this regard, the Kondo lattice model transforms to the model we studied in Ref. 7.

ACKNOWLEDGMENTS

I thank Patrick Lee for very useful discussions I have had with him about this and related issues and for encouraging me to write this paper. I am grateful for the conversations I had with Xiao-Gang Wen, Michael Hermele, Ying Ran, and Cody Nave. I am also grateful for the electronic mail exchanges I had with F. Guinea after this paper appeared on arXiv. The consideration of coherent Kondo couplings for plaquette impurities was especially motivated by his comment.

APPENDIX: INETGRAL TABLE

$$\int \frac{d^3k}{(2\pi)^3}\frac{k_\mu(k+q)_\nu}{k^2(k+q)^2}=\frac{-1}{64|q|}(q_\mu q_\nu+q^2\delta_{\mu\nu})+\cdots, \tag{A1}$$

$$\int_0^{2\pi}d\theta e^{ix\cos\theta}e^{in\theta}=2\pi i^n J_n(x), \tag{A2}$$

$$\lim_{\alpha\to\infty}\int_0^{\infty}dx x^2e^{-x/\alpha}J_0(x)=-1, \tag{A3}$$

$$\lim_{\alpha\to\infty}\int_0^{\infty}dx x^2e^{-x/\alpha}J_2(x)=+3, \tag{A4}$$

$$\lim_{\alpha\to\infty}\int_0^{\infty}dx x^2e^{-x^2/\alpha^2}J_0(x)=-1, \tag{A5}$$

$$\lim_{\alpha\to\infty}\int_0^{\infty}dx x^2e^{-x^2/\alpha^2}J_2(x)=+3. \tag{A6}$$

The ellipses in the first equation denote the nonuniversal pieces of the integral. They cause either exponential decay or faster algebraic decays in the continuum limit.

[1] S. Doniach, Physica B & C **91**, 231 (1977).
[2] A. Auerbach, *Interacting Electrons and Quantum Magnetism* (Springer, Berlin, 1994).
[3] K. S. Novoselov, A. K. Geim, S. V. Morozov, D. Jiang, M. I. Katsnelson, I. V. Grigorieva, S. V. Dubonos, and A. A. Firsov, Nature (London) **438**, 197 (2005).
[4] M. A. H. Vozmediano, M. P. Lopez-Sancho, T. Stauber, and F. Guinea, Phys. Rev. B **72**, 155121 (2005).
[5] V. K. Dugaev, V. I. Litvinov, and J. Barnas, Phys. Rev. B **74**, 224438 (2006).
[6] C. Kittel, *Quantum Theory of Solids* (Wiley, New York, 1987).
[7] S. Saremi and P. A. Lee, Phys. Rev. B **75**, 165110 (2007).
[8] T. Senthil, A. Vishwanath, L. Balents, S. Sachdev, and M. P. A. Fisher, Science **303**, 1490 (2004).